g Factor in Metallic Zinc*

ALAN J. BENNETT† AND L. M. FALICOV
Department of Physics and Institute for the Study of Metals, University of Chicago, Chicago, Illinois
(Received 26 June 1964)

A calculation of the g factor for the small "needles" of the Fermi surface of Zn has been carried on in the three-level approximation. It is shown that for fields parallel to the hexagonal axis, g is expected to be large with an upper bound of 133. This result rules out two of the three possibilities determined by Stark from experiment. It is found that three possible orderings of the levels can give the observed results, and the energy gaps are estimated in each case; the lattice potential and the spin-orbit splitting are of the same order of magnitude. The variation of the g factor with angle is in agreement with experiment.

1. INTRODUCTION

THE electronic properties of Zn have been the center of attention of many experimental[1–3] and theoretical[4] contributions. In particular some properties, like the de Haas–van Alphen effect[1,2] and the magnetoresistance[3] for fields parallel or nearly parallel to the hexad axis, seem to be dominated by two small pieces of electrons (the so-called "needles") in the third band. These pieces are located around the points K in the Brillouin zone (Fig. 1), contain on the whole about 5×10^{-6} electron per atom and have, perpendicular to the c axis, an area[2] of 0.00015 Å^{-2} with an effective cyclotron mass[3,5]

$$m^*=0.0075m_0 \tag{1}$$

(where m_0 is the free-electron mass).

The influence of these extremely small pieces appears to be enhanced when magnetic breakdown effects[3,6–8] are present. This is due to the fact that the quantized Landau levels of the "needles" modulate the transition probability between various pieces of Fermi surface, giving rise to strong oscillations in the magnetoresistance and the Hall effect which are periodic in $1/H$.

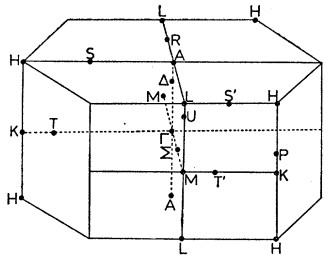

FIG. 1. The Brillouin zone in the hexagonal close-packed structure showing points and lines of symmetry.

This amplification of what would be otherwise rather weak de Haas–Schubnikov oscillations, results in the appearance of structure in the line shape and permits a more detailed analysis of the energy spectrum.

The experiments of Stark[3] in very pure samples, very carefully oriented, show, in addition to the expected "semiclassical" behavior due to magnetic breakdown,[9] strong doubly peaked oscillations with a period corresponding to the cross-sectional area of the "needles." Stark has attributed the double-peak structure to spin splitting; the energy levels which would reproduce the observed line shape are given by

$$E_n=(n+\gamma\pm\delta)\hbar\omega_c, \tag{2}$$

where

$$\omega_c=eH/m^*c, \tag{3}$$

m^* is given by (1), and the parameters γ and δ are one of the three possible combinations

$$\gamma=0.30 \quad \delta=\tfrac{1}{6}, \tag{4a}$$

$$\gamma=0.80 \quad \delta=\tfrac{1}{3}, \tag{4b}$$

$$\gamma=0.80 \quad \delta=\tfrac{2}{3}. \tag{4c}$$

The third term in (2) corresponds to the spin energy

$$E_s=\pm\tfrac{1}{2}g\mu_0H, \tag{5}$$

where μ_0 is the Bohr magneton. From (2), (3), and (5), the g factor is thus obtained from experiment by means of

$$|g|=4\delta m_0/m^*, \tag{6}$$

which corresponds, according to (1) and (4a), (4b), and (4c) to 89, 178, and 356, respectively.

Although so large a g factor is not uncommon in solids, e.g., bismuth,[10] it is surprising at first to see a free-electron-like metal like Zn display values so different from 2. However, it should be emphasized that

(a) the g factor under consideration corresponds not to the over-all Fermi surface, but specifically to the very small pieces centered about K;

* Supported in part by the National Science Foundation and the U. S. Office of Naval Research.
† National Science Foundation predoctoral fellow.
[1] See for instance, B. I. Verkin and I. M. Dmitrenko, Izvest. Akad. Nauk SSSR **19**, 409 (1955) [Columbia Tech. transl. **19**, 375 (1955)]; D. F. Gibbons and L. M. Falicov, Phil. Mag. **8**, 177 (1963); J. S. Dhillon and D. Shoenberg, Phil. Trans. Roy. Soc. (London) **A248**, 1 (1955).
[2] A. S. Joseph and W. L. Gordon, Phys. Rev. **126**, 489 (1962).
[3] R. W. Stark, Phys. Rev. **135**, A1698 (1964).
[4] W. A. Harrison, Phys. Rev. **126**, 497 (1962).
[5] F. T. Hedgcock and W. B. Muir, Phys. Rev. **129**, 2045 (1963).
[6] M. H. Cohen and L. M. Falicov, Phys. Rev. Letters **7**, 231 (1961); A. B. Pippard, Proc. Roy. Soc. (London) **A270**, 1 (1962).
[7] E. I. Blount, Phys. Rev. **126**, 1636 (1962).
[8] R. W. Stark, Phys. Rev. Letters **9**, 482 (1962).
[9] L. M. Falicov and P. R. Sievert, Phys. Rev. Letters **12**, 558 (1964).
[10] M. H. Cohen and E. I. Blount, Phil. Mag. **5**, 115 (1960).

(b) the very small effective mass (1) indicates the presence of some other levels very close in energy to the one under consideration;

(c) it has been shown previously[4] that the relevant lattice splittings are very small ($\sim$0.007 Ry) and of the same order of magnitude of the spin-orbit splittings[11] ($\sim$0.005 Ry).

Under these conditions a large g factor is likely to occur, as it has been previously found in other cases[10,12] and as the general theory of the behavior of Bloch electrons in a magnetic field[7] explicitly shows.

We have calculated the g factor for the third band at K following the formalism of Refs. 7 and 10, and assuming a three-band approximation. In Sec. 2 we discuss the details of the band structure around K both with and without spin-orbit effects. We show explicitly that the three-band approximation is very good for the present purposes although it fails in other hexagonal metals; the symmetry of the relevant states is fully analyzed.

In Sec. 3 the calculation of the g factor is carried on in detail; it is found that only (4a), i.e., $g=89$, is consistent with the theory. Three possible orderings of levels which correspond to such a value are discussed and the energy gaps estimated. Finally the calculated variation of g factor with angle is compared with preliminary experimental results.[13]

2. THE DETAILS OF THE BAND STRUCTURE AROUND K

In the absence of spin-orbit coupling, very general considerations show that the three bands of lowest energy at K are a doubly degenerate K_5 and a single K_1 level.[14] In the free-electron model these two coalesce in a 3-fold degenerate level with kinetic energy $E_k\approx0.70$ Ry. The actual ordering of this K_1-K_5 pair in Zn is in fact difficult to predict. Harrison[4] finds K_1 above K_5, but the splitting of 0.007–0.011 Ry is smaller than the estimated accuracy of a few hundredths of a rydberg. In addition, comparison with other hexagonal metals shows K_1 and K_5 in thallium,[15] with an energy gap of 0.125 Ry, and K_5 above K_1 in magnesium,[16] with an energy gap of 0.04 Ry, that is, a trend for K_1 to increase and be above K_5 as the atomic number increases, with Zn being probably a borderline case. The next set of levels, K_2, K_3, K_5, and K_6, has an average kinetic energy $E_k\approx1.17$ Ry, i.e., they are separated from the relevant set by an average of 0.47 Ry.

When spin-orbit coupling is taken into account, the K_1 state becomes K_7 in character and the K_5 state is split into K_8 and K_9 representations.

The splitting of the K_8 and K_9 levels can be estimated by scaling the known value of the corresponding splitting in Mg.[17] The scaling factor taken from the corresponding atomic term values[18] is 9.5 and gives K_8 above K_9 with an energy difference of 2.7×10^{-3} Ry. In addition, a tight-binding approximation in the spin-orbit calculation gives a splitting equal to $\frac{2}{3}\Delta$, where Δ is the $J=\frac{3}{2}$, $J=\frac{1}{2}$ splitting in the atom. Since $\Delta=7.95\times10^{-3}$ Ry,[18] this approach gives a splitting of 5.3×10^{-3} Ry. So, within a factor of 2, the spin-orbit-induced gap is known; we can therefore take the value of Δ as our unit and correspondingly scale all energies when Δ is readjusted.

In order to compute the effective masses and the g factor at K, we have made use of the $\mathbf{k}\cdot\mathbf{p}$ perturbation theory, suitably generalized to include spin, i.e., we need to know the interband matrix element of the velocity operator

$$\mathbf{v}=(1/m_0)\mathbf{p}+(1/2m_0c^2)\mathbf{s}\times\nabla V, \tag{7}$$

where $\mathbf{p}$ is the momentum, $\mathbf{s}$ the spin and V the lattice potential.

The well-known formula for the inverse effective-mass tensor at a given point of a band o,

$$^{o}\left(\frac{1}{m_{ij}}\right)=\frac{\delta_{ij}}{m_0}+\sum_n\frac{\langle o|v_i|n\rangle\langle n|v_j|o\rangle+\langle o|v_j|n\rangle\langle n|v_i|o\rangle}{E_o-E_n}, \tag{8}$$

clearly points out that in order to get a cyclotron mass as small as (1), it is necessary to have, very close in energy to the band o under consideration, at least one additional band of lower energy. Since the next upper bands are on the average about 0.4 Ry apart, they can only contribute a very small amount to the effective mass and g factor at K, and consequently can be neglected for the present purposes.

The value of the de Haas–van Alphen period together with the cyclotron mass indicates that the Fermi energy lies only about 0.0018 Ry above the third K level. As a consequence (a) the effective mass and g factor computed at K should be a good approximation throughout the "needle," (b) the third band can be considered parabolic for all practical purposes, and (c) the three-band approximation is certainly a good one. It should be noted in passing that this only holds for Zn because in the other hexagonal-close-packed metals the third level has moved well below the Fermi energy (Mg,[16] Tl[15]) or well above it (Cd [1]).

In order to compute the matrix elements of (7), it is necessary first to specify the functions corresponding

[11] M. H. Cohen and L. M. Falicov, Phys. Rev. Letters **5**, 544 (1960); and L. M. Falicov and M. H. Cohen, Phys. Rev. **130**, 921 (1963).
[12] J. M. Luttinger, Phys. Rev. **102**, 1030 (1956).
[13] W. L. Gordon (private communication).
[14] For the notation and character tables of the small groups of the hexagonal-close-packed structure, see C. Herring, J. Franklin Inst. **233**, 525 (1942), and R. J. Elliott, Phys. Rev. **96**, 280 (1954).
[15] P. Soven (private communication, to be published).
[16] L. M. Falicov, Phil. Trans. Roy. Soc. (London) **A255**, 55 (1962).
[17] M. G. Priestley, L. M. Falicov, and G. Weisz, Phys. Rev. **131**, 617 (1963).
[18] Charlotte E. Moore, Natl. Bur. of Std. (U.S.) Circ. No. 467 (1949).

TABLE I. Angular-momentum character of the wave functions about the lattice sites and the center of symmetry.

	Atom 1	Atom 2	Center of symmetry
$\|1\rangle$	ip_x-p_y	ip_x+p_y	s
$\|a\rangle$	s	ip_x-p_y	ip_x+p_y
$\|b\rangle$	ip_x+p_y	s	ip_x-p_y

to the K_1 (K_7) and K_5 (K_8, K_9) levels. Group-theoretical arguments tell immediately which of these matrix elements are nonzero. It is convenient, however, for making arguments more explicit, to give as an example the following combination of plane waves [or orthogonalized plane waves (OPW)] which have the required symmetry[19]:

$$\begin{aligned}|1\rangle&=|k_1\rangle+\omega^2|k_2\rangle+\omega|k_3\rangle,\\ |a\rangle&=|k_1\rangle+|k_2\rangle+|k_3\rangle,\\ |b\rangle&=|k_1\rangle+\omega|k_2\rangle+\omega^2|k_3\rangle.\end{aligned}\tag{9}$$

Here $\omega=-\frac{1}{2}+i(\sqrt{3}/2)$, $|k_i\rangle$ represent plane waves (or OPW's) with k vectors defined in Fig. 2; $|1\rangle$ transforms according to the K_1 representation while $|a\rangle$ and $|b\rangle$ transform according to K_5. Of course any linear combinations of $|a\rangle$ and $|b\rangle$ also transform according to K_5, but the present choice is the most convenient, since when spin-orbit coupling is taken into account and the spin is quantized along the hexad axis,

$|1\uparrow\rangle$ and $|1\downarrow\rangle$ transform according to K_7,

$|a\uparrow\rangle$ and $|b\downarrow\rangle$ transform according to K_8,

$|b\uparrow\rangle$ and $|a\downarrow\rangle$ transform according to K_9.

These properties can be clearly seen from the angular-momentum character of the wave functions (9) about the lattice sites. This information can be obtained from the transformation properties of the functions or, more easily, by expanding them in power series in $\mathbf{r}$ around the corresponding points. The s- and p-like contributions are listed in Table I.

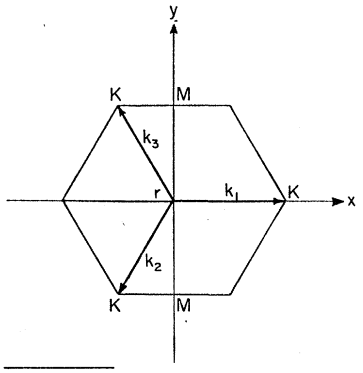

FIG. 2. The first three k vectors contributing to the wave functions at K.

[19] It should be understood the functions shown in (9) are not those actually used in computations. In fact all the arguments following should be interpreted as referring to general functions which have the same symmetry as $|1\rangle$, $|a\rangle$, and $|b\rangle$.

The energy of the relevant levels will be specified by two parameters E and Δ such that

$$\begin{aligned}E_7&=0,\\ E_8&=E+\Delta/3,\\ E_9&=E-\Delta/3.\end{aligned}\tag{10}$$

E can have either sign, but Δ, the "atomic" spin-orbit splitting, is defined positive. This implies that only K_7 or K_8 can be the (third) level corresponding to the "needle," depending on whether E is larger or smaller than $-\Delta/3$.

The velocity operator (7) can be divided into a "spinless" part $\mathbf{P}=(1/m_0)\mathbf{p}$ and a spin-orbit part $\mathbf{R}=(1/2m_0^2c^2)\mathbf{s}\times\nabla V$. Symmetry considerations show that many of the matrix elements are zero, and those which do not vanish can be expressed in terms of three parameters A, B, and C which are real. Tables II and III give the matrix elements of P_x, P_y, P_z and R_x, R_y, R_z, respectively. It should be noted that: (a) in general, A and B are expected to be much greater than C, which is only a relativistic correction; (b) A and B are of the same order of magnitude, and in fact in the three-plane-wave approximation $A=B$; (c) since the spin-orbit Hamiltonian is a function of $\mathbf{P}$ and $\mathbf{R}$,

$$\mathcal{H}_{so}=(1/2m_0^2c^2)\mathbf{p}\cdot\mathbf{s}\times\nabla V=m_0\mathbf{P}\cdot\mathbf{R},\tag{11}$$

in the three-band approximation

$$6m_0AC=\Delta\tag{12}$$

as can be easily seen from (11), (10), and Tables II and III.

Having defined the matrix elements of the velocity, the application of (8) to the K_7 and K_8 levels gives:

$$^7\left(\frac{m_0}{m_{xx}}\right)=^7\left(\frac{m_0}{m_{yy}}\right)=1-\frac{2m_0(A-C)^2}{E-\Delta/3}-\frac{2m_0(A+C)^2}{E+\Delta/3},\tag{13}$$

$$^7\left(\frac{m_0}{m_{zz}}\right)=1-\frac{8m_0C^2}{E+\Delta/3},\tag{14}$$

$$^8\left(\frac{m_0}{m_{xx}}\right)=^8\left(\frac{m_0}{m_{yy}}\right)=1+\frac{2m_0(A+C)^2}{E+\Delta/3}+\frac{3m_0B^2}{\Delta},\tag{15}$$

$$^8\left(\frac{m_0}{m_{zz}}\right)=1+\frac{8m_0C^2}{E+\Delta/3}.\tag{16}$$

TABLE II. Matrix elements of the "spinless" velocity operator $\mathbf{P}=\mathbf{p}/m$.

	P_x			P_y			P_z
	$1\|\rangle$	$\|a\rangle$	$\|b\rangle$	$\|1\rangle$	$\|a\rangle$	$\|b\rangle$	
$\langle 1\|$	0	A	A	0	$-iA$	iA	All zero
$\langle a\|$	A	0	B	iA	0	$-iB$	
$\langle b\|$	A	B	0	$-iA$	iB	0	

TABLE III. Matrix elements of the spin part of the velocity operator. $\mathbf{R}=\mathbf{s}\times\nabla V/2m^2c^2$.

	R_x						R_y						R_z					
	$\|1\uparrow\rangle$	$\|1\downarrow\rangle$	$\|a\uparrow\rangle$	$\|b\downarrow\rangle$	$\|b\uparrow\rangle$	$\|a\downarrow\rangle$	$\|1\uparrow\rangle$	$\|1\downarrow\rangle$	$\|a\uparrow\rangle$	$\|b\downarrow\rangle$	$\|b\uparrow\rangle$	$\|a\downarrow\rangle$	$\|1\uparrow\rangle$	$\|1\downarrow\rangle$	$\|a\uparrow\rangle$	$\|b\downarrow\rangle$	$\|b\uparrow\rangle$	$\|a\downarrow\rangle$
$\langle 1\uparrow\|$	0	0	C	0	$-C$	0	0	0	$-iC$	0	$-iC$	0	0	0	0	$2C$	0	0
$\langle 1\downarrow\|$	0	0	0	C	0	$-C$	0	0	0	iC	0	iC	0	0	$-2C$	0	0	0
$\langle a\uparrow\|$	C	0	0	0	0	0	iC	0	0	0	0	0	0	$-2C$	0	0	0	0
$\langle b\downarrow\|$	0	C	0	0	0	0	0	$-iC$	0	0	0	0	$2C$	0	0	0	0	0
$\langle b\uparrow\|$	$-C$	0	0	0	0	0	iC	0	0	0	0	0	0	0	0	0	0	0
$\langle a\downarrow\|$	0	$-C$	0	0	0	0	0	$-iC$	0	0	0	0	0	0	0	0	0	0

We are interested in (13) and (14) for $E<-\Delta/3$, and (15) and (16) for $E>-\Delta/3$. In either case, since $m_{xx}=m_{yy}$, (13) or (15) should be equal to m_0/m^*, i.e., 133. With this in mind, and by neglecting terms of the order C^2 and using the definitions, we obtain

$$\xi=E/\Delta \quad \alpha=m_0A^2/\Delta>0 \quad \beta=m_0B^2/\Delta>0. \quad (17)$$

Equations (13)–(16) can be simplified to

$$^7\left(\frac{m_0}{m_{xx}}\right)=^7\left(\frac{m_0}{m_{yy}}\right)\approx-\frac{4\xi\alpha}{\xi^2-\frac{1}{9}}\approx\frac{m_0}{m^*}, \quad \xi<-\tfrac{1}{3}, \quad (18)$$

$$^8\left(\frac{m_0}{m_{xx}}\right)=^8\left(\frac{m_0}{m_{yy}}\right)\approx\frac{2\alpha+\beta+3\beta\xi}{\xi+\frac{1}{3}}\approx\frac{m_0}{m^*}, \quad \xi>-\tfrac{1}{3}, \quad (19)$$

$$^7\left(\frac{m_0}{m_{zz}}\right)\approx^8\left(\frac{m_0}{m_{zz}}\right)\approx1. \quad (20)$$

3. THE CALCULATION OF THE g FACTOR

In what follows we calculate the g factor according to theory of Cohen and Blount[10] and Blount.[7] The effective-mass Hamiltonian for the relevant spin-degenerate band in the presence of a magnetic field is given by

$$\langle s|\mathcal{H}|s'\rangle^o=\left\{\frac{\hbar^2}{2m^*}\left[\left(k_x-\frac{e}{c\hbar}A_x\right)^2+\left(k_y-\frac{e}{c\hbar}A_y\right)^2\right]+\frac{\hbar^2}{2m_{zz}}\left(k_z-\frac{e}{c\hbar}A_z\right)^2+E_o\right\}\delta_{ss'}-\langle s|\mathbf{u}|s'\rangle^o\cdot\mathbf{H}. \quad (21)$$

Here s and s' indicate the spin states in the degenerate band, o indicates K_7 (if $E>-\Delta/3$) or K_8 (if $E<-\Delta/3$), E_8 is given by (10), and $\mathbf{u}$ is the intrinsic magnetic moment of the electron, consisting of an orbital part $\mathbf{u}_l$ and a spin part $\mathbf{u}_s$

$$\mathbf{u}=\mathbf{u}_l+\mathbf{u}_s, \quad (22)$$

$$\mathbf{u}_s=-2\mu_0\mathbf{s}. \quad (23)$$

The expression for $\mathbf{u}_l$, which is due to the unquenched orbital motion, is[10]

$$\langle s|\mathbf{u}_l|s'\rangle^o=-\frac{e\hbar}{2ci}\sum_{ns''}\frac{\langle 0s|\mathbf{v}|ns''\rangle\times\langle ns''|\mathbf{v}|0s'\rangle}{E_0-E_n}, \quad (24)$$

where n represents all other bands.

By means of (7), (10), and Tables II and III, (24) can be straightforwardly computed, with the results

$$^7\left(\frac{\mu_x}{\mu_0}\right)=-^8\left(\frac{\mu_x}{\mu_0}\right)=\frac{2m_0C(A+C)}{E+\Delta/3}\sigma_x\approx\frac{1}{3\xi+1}\sigma_x, \quad (25)$$

$$^7\left(\frac{\mu_y}{\mu_0}\right)=^8\left(\frac{\mu_y}{\mu_0}\right)=\frac{2m_0C(A+C)}{E+\Delta/3}\sigma_y\approx\frac{1}{3\xi+1}\sigma_y, \quad (26)$$

$$^7\left(\frac{\mu_z}{\mu_0}\right)=\left[\frac{m_0(A+C)^2}{E+\Delta/3}+\frac{m_0(A-C)^2}{E-\Delta/3}\right]\sigma_z\approx\frac{2(\xi-\alpha)}{3\xi^2-\frac{1}{3}}\sigma_z, \quad (27)$$

$$^8\left(\frac{\mu_z}{\mu}\right)=\left[\frac{m_0(A+C)^2}{E+\Delta/3}-\frac{3m_0B^2}{2\Delta}\right]\sigma_z\approx\left[\frac{\alpha}{\xi+\frac{1}{3}}-\frac{3\beta}{2}\right]\sigma_z, \quad (28)$$

where σ_x, σ_y, σ_z are the Pauli matrices, and the last expressions are obtained with similar approximations to those which led to (17)–(20). It is interesting to point out that all components of the magnetic moment can be expressed in terms of the Pauli matrices without

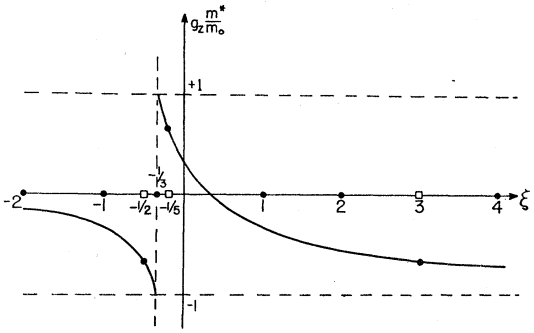

FIG. 3. The g factor as a function of $\xi=E/\Delta$.

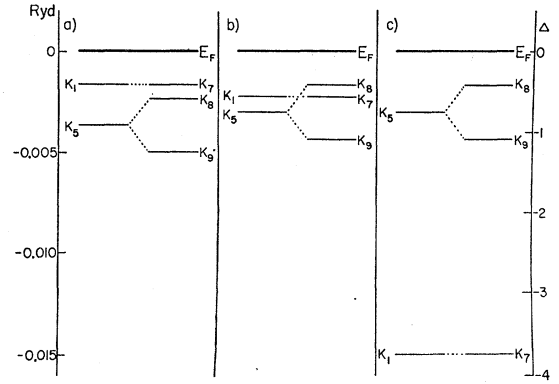

FIG. 4. The three possible orderings of levels which correspond to a g factor of 89.

any contribution of the unit matrix; this means that no magnetic moment is apparent in this approximation.[20]

We now analyze the case in which the magnetic field is parallel to the hexagonal axis. In that case $g_z=2(\mu_z/\mu_0)$; from (18) and (27) the parameter α can be eliminated and

$$g_z m^*/m_0 \approx 1/3\xi, \quad \xi<-\tfrac{1}{3}. \tag{29}$$

This function is plotted in the left-hand portion of Fig. 3, and it is seen that it can only vary between 0 and -1, giving $|g|<133$.

The same condition $|g|<133$ can be obtained from (19) and (28) by requiring $\alpha>0, \beta>0$. As a consequence, only one of the three possible experimental values (4), namely (4a), is compatible with this calculation. The variation of g_z with the energy difference between K_1 and K_5 cannot be explicitly found if no relation between α and β (i.e., A^2 and B^2) is known. For the sake of clarity, and in order to give an explicit example, we have assumed the relation satisfied by the linear combinations of three plane waves, namely $\alpha=\beta$. In that case, by eliminating α between (19) and (28) we obtain

$$g_z m^*/m_0 \approx (-3\xi+1/3\xi+3), \quad \xi>-\tfrac{1}{3}. \tag{30}$$

[20] *Note added in proof.* The hexagonal-close-packed structure possesses a center of inversion and consequently shows no magnetic moment. However, the pieces centered about K are *not* symmetric under inversion individually; this results in a nonzero magnetic moment corresponding to *each* piece for fields in arbitrary directions. The total moment of the *two* "needles," which are related by inversion, is on the other hand exactly zero.

This function varies between -1 and $+1$ and it is plotted in the right-hand side of Fig. 3.

We can now assume that the experimental value $|g_z m^*/m_0|=\frac{2}{3}$ is the right one, and determine from (29) and (30) the various possibilities for the ordering of levels. The three possible values for ξ are -0.5, -0.2, and $+3$, which from (17) and (10) correspond to three orderings shown in Fig. 4. It is interesting to note that in every case E and Δ are of the same order of magnitude, i.e., the energy gap due to the lattice potential is as small as the spin-orbit splitting. We are now in a position to study the variation of the g factor with angle, i.e., the energy splitting of the two spin levels when the magnetic field is rotated off the hexagonal axis. A diagonalization of the $\mathfrak{y}\cdot\mathbf{H}$ term of (21) for H forming an angle θ with the sixfold axis yields an energy difference E_M between the two spin states which in turn gives a g factor

$$g(\theta)=\left[(g_z\cos\theta)^2+\left(\frac{2\sin\theta}{3\xi+1}\right)^2\right]^{1/2}. \tag{31}$$

For the three values of ξ chosen to give $g_z=89$, the second term in (31) is much smaller than the first for all angles up to, say, 70°; this gives for the g factor a $\cos\theta$ variation.

This result is in agreement with preliminary experimental information[13] based on a detailed study of the line shape of the de Haas–van Alphen oscillations in the "needle." This analysis shows that, within experimental error the product of g and the cyclotron mass m_c is independent of orientation for magnetic fields not too close to the basal plane. It is also known from experiment[2] that m_c varies very nearly like the secant of the angle θ.

ACKNOWLEDGMENTS

The authors are grateful to Dr. R. W. Stark and Dr. W. L. Gordon for several enlightening discussions on their experiments and to P. Soven for interesting remarks.

In addition to the direct support by the National Science Foundation and the Office of Naval Research, this research has benefited indirectly from support to the Institute for the Study of Metals by the National Science Foundation and the Advanced Research Projects Administration.